



## Investigation of in vitro toxicity of newly synthesized mesoporous silica nanotubes with different pore sizes in human liver cancer cells (HepG2)

Hasan ULUSAL<sup>1,\*</sup>, Fatma ULUSAL<sup>2</sup>

<sup>1</sup>Department of Medical Biochemistry Health. Sciences Institute, Gaziantep University, 27310, Gaziantep, Türkiye

<sup>2</sup>Department of Chemistry and Chemical Processing Technologies, Tarsus University, 33100, Mersin, Türkiye

Received: 6 June 2024; Revised: 12 August 2024; Accepted: 15 August 2024

\*Corresponding author e-mail: [hasan\\_ulusal@hotmail.com](mailto:hasan_ulusal@hotmail.com)

**Citation:** Ulusal, H.; Ulusal, F. *Int. J. Chem. Technol.* 2024, 8 (2), 1035-113

### ABSTRACT

Nanotechnology has gained importance in recent years with the use of nanomaterials smaller than human cells in many areas such as food, cosmetics, defense industry and pharmaceutical industry. It has begun to be widely used in the field of health in the diagnosis and treatment of many diseases, especially cancer. However, due to their size and content, these materials can be toxic and pose a risk to human health. In this study, the cytotoxic effects of mesoporous silicon dioxide (SiO<sub>2</sub>) nanoparticles with different pore sizes, synthesized using a new method and made from polyethylene glycol 6000 (PEG6000) and polyethylene glycol 35000 (PEG35000) were tested on HepG2 cells liver carcinoma cells. Additionally, the effects of mesoporous silica nanotubes on lipid peroxidation and reactive oxygen species (ROS) were also examined. It was found that the cytotoxicity of both types of mesoporous SiO<sub>2</sub> nanoparticles increased with rising concentration. Cell viability decreased significantly as the nanoparticles dosage (100-10 µg/mL) increased. Both nanoparticles were not cytotoxic at concentrations up to 50 µg/mL, however, they became cytotoxic at higher concentrations (p<0.05). The toxic effect at higher concentrations is thought to be due to increased intracellular SiO<sub>2</sub> concentrations. The results indicated that these nanomaterials can be used as a good drug carrier at certain concentrations because they are both safe, inexpensive and easy to synthesize.

**Keywords:** Cytotoxicity, HepG2 cell line, Mesoporous silica, Polyethylene glycol.

### 1. INTRODUCTION

Silica, also commonly known as silicon dioxide (SiO<sub>2</sub>), is an oxide of semi-metal found in both amorphous and crystalline forms. There are many different types of crystalline silica, including moganite, β-crystobalite, stishovite, β-tridymite, β-quartz, α-quartz, α-tridymite, α-crystobalite, coesite and keatite. The most common form of crystalline silica is α-quartz, which is often referred to simply as "quartz." Inhaling crystalline form of silica through the use of products containing quartz form is the primary way that the general population is exposed to this substance. Some common products that contain quartz and may be used by the general population include cleaning agents, paint, putty, caulk, talcum powder, pet litter, cosmetics, artistic clays and glazes, and grout. The common population may also be exposed to quartz through ingestion of drinking water, although there is no data available on the levels of exposure that may occur through this route. <sup>1,2</sup>

Silica is a widely used material in various fields, including mechanical and chemical polishing, cosmetics, pharmaceuticals, toner printers, varnishes, and food. <sup>3</sup> However, in recent years, nanosized silica has gained particular interest in biomedicine and biotechnology, such as in biosensors, enzyme immobilization, cancer biomarkers, DNA carriers, cancer therapy, and drug carriers. <sup>3-5</sup> It is increasingly being used in the coating of nanomaterials due to its unique properties, which are due to its large surface area and differ significantly from those of microscale particles. Silica has also gained attention due to its potential environmental and health effects. Exposure to microsilica has been linked to the improvement of various autoimmune diseases, including lupus, rheumatoid arthritis, systemic sclerosis, and chronic kidney disease. Moreover, crystalline polymorphs of silica can cause lung cancer and silicosis <sup>6-8</sup>.

Nanosized SiO<sub>2</sub> has been shown to cause fibrogenesis in mice, proinflammatory stimulation of endothelial cells,

and abnormal topoisomerase I clusters in the nucleoplasm of cells, though some *in vivo* studies in mice have found that SiO<sub>2</sub> nanoparticles (NTPs) are non-toxic.<sup>9-11</sup> However, more researches are needed to fully understand the toxic effects of silica NTPs on human health and the mechanisms behind these effects.<sup>12</sup> Mesoporous SiO<sub>2</sub> nanoparticles have also been used for intravenous or oral administration in diseases such as cancer and Alzheimer's disease, though the cell/tissue/organism-level toxicity and co-destruction with double-covered nanoparticles are still areas of ongoing research. Chauhan et al. have conducted a systematic study of the toxicity of mesoporous SiO<sub>2</sub> at the cell level in a dose-dependent manner.<sup>13</sup>

Nanotechnology has become increasingly important in the last years, with several nanomaterials that are smaller than human cells being widely used in food packaging, sunscreens, cosmetics, pharmaceuticals, and the diagnosis and treatment of diseases, particularly cancer types. However, these materials can be toxic and pose a risk to human health and safety due to their size and composition. Therefore, it is very important to evaluate the potential toxic effects of nano-sized particles before using. Traditionally, toxicity studies have been elaborated using animals to assess the potential harmful effects of nanomaterials and chemicals on humans.<sup>14</sup> However, there is growing pressure to reduce the use of animals in such studies, particularly in the US and Europe, due to ethical concerns.<sup>15</sup> As a result, there is a need for alternative test methods that can accurately predict nanomaterial toxicity. One such method is the use of human cell models, which are cost-effective, easy to use, and highly reproducible, and can help reduce unnecessary animal testing.<sup>14</sup>

When a nanoparticle is first prepared, its cytotoxic effects must be examined, especially before it is used in the medical field. Nanoparticles that are not toxic to cells and tissues can be used as safe mediators in the health field. The nanoparticles we prepared have not been used in the literature before. In addition, there is no study examining the cytotoxic effects of two nanoparticles prepared with different polymers (PEG6000 and PEG350000) and different sizes. In this current research, the cytotoxic effects of mesoporous SiO<sub>2</sub> nanoparticles, synthesized using a new technique, were investigated in a dose-dependent behavior in the HepG2 cell line, and their effects on lipid peroxidation and reactive oxygen species (ROS) were also examined. We hypothesize that mesoporous silica nanotubes synthesized with PEG6000 and PEG35000 will exhibit distinct cytotoxic profiles in HepG2 cells, with variations in pore size influencing their impact on cell viability, ROS production, and lipid peroxidation.

## 2. MATERIALS AND METHODS

### 2.1. Materials

General spectroscopic methods were used for the characterization of the prepared materials. Polyethylene glycols have an average weight of 6000 kDa and 35000 kDa. Dimethyl sulfoxide (DMSO), 2-thiobarbituric acid (TBA), sodium hydroxide (NaOH), trichloroacetic acid (TCA), phosphate buffer saline (PBS), Ethylenediaminetetraacetic acid (EDTA) and 2',7'-dichlorofluorescein diacetate (DCFH-DA) were obtained from Sigma-Aldrich. All materials were used without further purification. Gaziantep University Medical Biochemistry Department provided a HepG2 cell line. Fetal bovine serum and DMEM medium were purchased from Capricorn.

### 2.2. Method

The effects of mesoporous SiO<sub>2</sub>-(PEG6000) and SiO<sub>2</sub>-(PEG35000) nanotubes, synthesized, and characterized herein, were examined in the HepG2 cell line to determine whether they were suitable for cell and animal studies. For this purpose, MTT cytotoxicity analysis and reactive oxygen species (ROS) measurement in nanotube-applied cells and malondialdehyde (MDA) measurement in cell homogenate were performed. Field Emission Scanning Electron microscope (FE-SEM) image was taken on the ZEISS brand GEMINI 500 model device. High-resolution Transmission Electron Microscopy (HR-TEM) analysis was taken on a JEOL brand JEM 2100F model Transmission Electron Microscope with a FEG electron gun operating under accelerating voltage in the range of 80-200 kV. X-ray Diffraction (XRD) analysis Rigaku Miniflex CuK $\alpha$ ,  $\lambda=0.154$  nm instrument was used, and analysis was performed in the range of  $2\theta=10-90^\circ$ .

### 2.3. Mesoporous silica synthesis

The general method for the preparation of mesoporous SiO<sub>2</sub> is given in Figure 1. To prepare mesoporous silica, the compound of polyethylene glycol with a molecular weight of 6000 kDa (PEG6000) or 35000 kDa (PEG35000) was mixed in 6% hydrochloric acid (HCl) solution, with a ratio of 3.2% in the final solution. The solution temperature was brought to 40°C and stirred magnetically until completely a clear solution was obtained. Tetraethoxy silane (TEOS) was added to the transparent solution obtained, 2.3 times by mass of the PEG6000 compound used, and this solution was maintained at 40°C for 24 hours. Then, the whitish mixture was brought to 80 °C and stirred under reflux for 60 hours under these experimental conditions. The product in the form of white powder was brought to room temperature after 60 hours and centrifuged. It was washed with pure water until its pH value became neutral. The resulting white powder product was firstly dried in an oven at 60 °C for 12 h, then burned in a 550 °C furnace for 6 hours under atmospheric pressure. The white powder obtained was analyzed by methods according to Lin et al.<sup>4</sup>

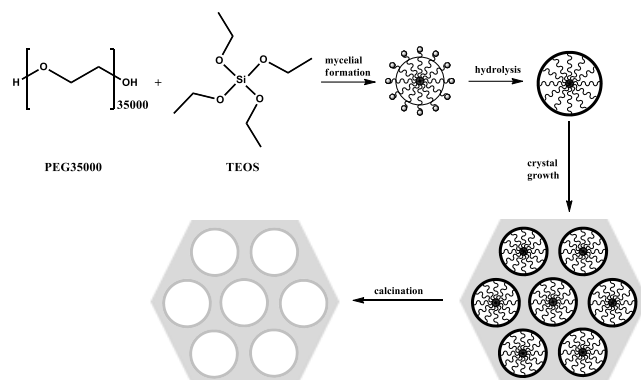


**Figure 1.** Synthesis of mesoporous silica.

#### 2.4. Thiazolyl blue tetrazolium bromide (mtt) cytotoxicity analysis

HepG2 cells with passage numbers of 12-15 were used for cytotoxicity analysis. When HepG2 cells reached a sufficient number, they were counted and seeded in 24-well plates with nearly  $15 \times 10^4$  cells in each well. The cells were cultivated in DMEM medium containing 1% penicillin and 10% FBS and incubated for two days in a CO<sub>2</sub> incubator at 37°C, 95% humidity, and 5% CO<sub>2</sub>. Then, the medium was taken and DMEM medium was added to it. Mesoporous SiO<sub>2</sub> was prepared at final concentrations of 10, 25, 50 and 100 µg/mL and added to the wells in 4 repetitions. Concentrations were selected by taking into account studies in the literature.<sup>16, 17</sup> Cells in DMEM medium without mesoporous SiO<sub>2</sub> nanotubes were used as controls. Cells were treated with mesoporous SiO<sub>2</sub> nanotubes at various concentrations for 24 and 48 hours, the MTT solution to be 5 mg/mL in the final solution was placed in the wells, and the result solution was incubated for 4 hours in the incubator. Subsequently, the cell medium was carefully taken, 1000 µL of DMSO was added to the wells, mixed, and 10 minutes later, a reading was performed in a microplate reader at 570 nm. The viability of the control cell was assumed to be 100% and the viability calculation was made for the drug-treated cells. Since no effect was observed in 24-hour applications, subsequent procedures will be applied within a 48-hour incubation period.

#### 2.5. Intracellular reactive oxygen species (ROS)

The ROS production was determined using DCFH-DA.<sup>18</sup> It is known that DCFH-DA passively enters the cell where a reaction with ROS results in a highly fluorescent chemical called dichlorofluorescein (DCF). In this study, a 10 mM stock solution of DCFH-DA prepared in methyl alcohol was diluted 500-fold in HBSS (Hank's Balanced Salt Solution) to yield a 20 µM working solution without the addition of serum or other additives. After the cells (in the 24-well plate) were exposed to mesoporous silica NTPs for 48 h, they were washed three times with HBSS, after then result solution incubated in 2 mL solution of 20

µM DCFH-DA at 37 °C for 30 min. Then, the fluorescence of samples was measured at 520 nm emission and 485 nm excitation using a microplate reader. ROS test was applied for the detection of reactive oxygen species. For this purpose, cells treated with NTPs at 10, 25, 50, and 100 µg/mL concentrations were isolated and ROS measurement was made. Results were compared to control.

#### 2.6. Malondialdehyde (MDA)

The levels of MDA were measured based on the working principles described by Jain et al.<sup>19</sup> To summarize briefly, 0.025 mL of butylated hydroxytoluene (BHT), 0.8 mL of phosphate buffer and 0.5 mL of trichloroacetic acid (TCA) were placed to 0.2 mL of cell conjugate. The tubes were vortexed and kept at -20 °C for 2 h. And then, it was centrifuged at 2000 rpm for at least 15 min. As a result of these processes, 1.0 mL of the supernatant sample was taken into a new test tube, 0.075 mL 0.1M EDTA, and 0.25 mL TBA dissolved in 1% 0.05N sodium hydroxide solution were added. The sample tube was then vortexed and incubated at 100 °C in a water bath for 20 min. Then, the temperature of the tubes was expected to drop to room temperature by itself. The absorbance of samples was determined at 532 nm using a UV-Vis spectrometer. MDA levels were calculated using the molar absorption coefficient ( $1.6 \times 10^5 \text{ cm}^{-1}\text{M}^{-1}$ ). MDA test was performed on cells treated with mesoporous SiO<sub>2</sub>. For this purpose, cells that were treated with nanoparticles at 10, 25, 50, and 100 µg/mL concentrations were isolated, and MDA was measured.

#### 2.7. Determination of protein

Protein determination in cell conjugate was measured in the Biotek H1 Synergy (USA) instrument using a Taken 3 plate. Results were calculated as mg/mL.

#### 2.8. Statistical analysis

Statistical analysis of the results was calculated with computer-assisted SPSS 22.0 test. The results obtained at different concentrations were compared with the control group containing only the medium (negative control). All analyses were performed in 4 replicates. 100 µM H<sub>2</sub>O<sub>2</sub> was used as the positive control group. One way ANOVA test was used for comparison between groups. Tamhane Post Hoc test was preferred for the analysis of normally distributed data. Tukey-HSD Post Hoc test was preferred for the analysis of data that showed abnormal distribution. The statistical significance level was accepted as  $p < 0.05$  and the comparison was made accordingly.

### 3. RESULTS AND DISCUSSION

#### 3.1. Material characterization

Polyethylene glycol 6000 is an organic polymer and is a polymeric material consisting of 6000 monomers. When the appropriate amount of PEG6000 is mixed in a solution containing HCl, it forms a micelle structure. It is ensured that the PEG structure forms a micelle structure by forming  $-OH^{2+}$  ends by the addition of concentrated HCl. Then, it imitates the structure created by PEG6000 by wrapping around the micelles formed when TEOS is added. After the heat application, the white powder material separated from the environment by centrifugation was dried at 60 °C overnight, and then incineration was carried out in the furnace. The purpose of this process is the separation of PEG residues trapped in the material by burning. As a result of this process,  $SiO_2$  in a mesoporous structure with a white powder appearance was obtained. FT-IR, BET, and XRD analysis were performed in the characterization of this material.

Figure 2 shows the FT-IR spectrum of mesoporous  $SiO_2$  prepared from PEG6000. The intense peak observed at  $1001.9\text{ cm}^{-1}$  in the FT-IR spectrum indicates the Si-OH peak. The broad peak observed at  $3364.4\text{ cm}^{-1}$  indicates the O-H peak. The O-H group obtained in both peaks originates from the naturally occurring OH group on the surface of mesoporous  $SiO_2$ . However, the expected Si-O-Si, Si-Si, and Si-O peaks in the range of 800-900 could not be observed because the vibration peak observed at  $1001.9\text{ cm}^{-1}$  was very broad. <sup>20</sup>

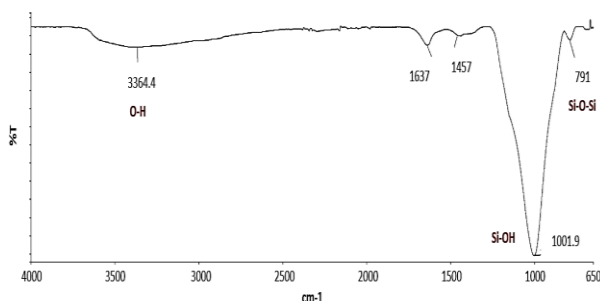


Figure 2. FT-IR spectrum of mesoporous  $SiO_2$  from PEG6000.

Figure 3 shows the XRD diffraction pattern of mesoporous  $SiO_2$  from PEG6000 (a) and PEG35000 (b). The peaks obtained in the range of  $2\theta$ :  $13-38^\circ$  are the main peaks of  $SiO_2$  with amorphous properties. As the peaks in the XRD spectrum become sharper and the intensity value increases, it shows that this substance moves toward the crystal structure. The results of the XRD spectrum comply well with the studies in the literature, therefore it can be said that the desired structure was obtained. <sup>20</sup>

The SEM image of mesoporous  $SiO_2$  obtained from PEG6000 is given in Figure 4. It is seen that the structure formed has very homogeneous dimensions. The material used as a template in the next stages was porous and agglomeration was not observed. Based on the SEM images, it is seen that the targeted material has been

synthesized. The size of the material to be prepared is expected to be below a few micrometers, as it is intended for use in application areas such as drug transport and catalyst support material.

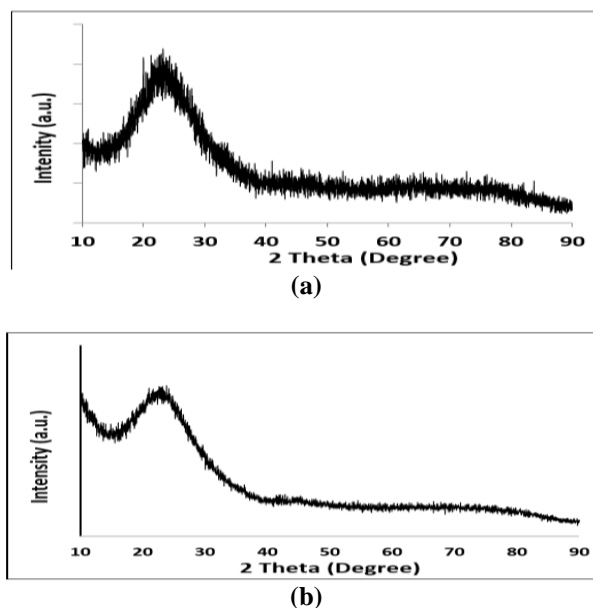


Figure 3. XRD diffraction patterns of mesoporous  $SiO_2$  from PEG6000 (a) and PEG35000 (b).

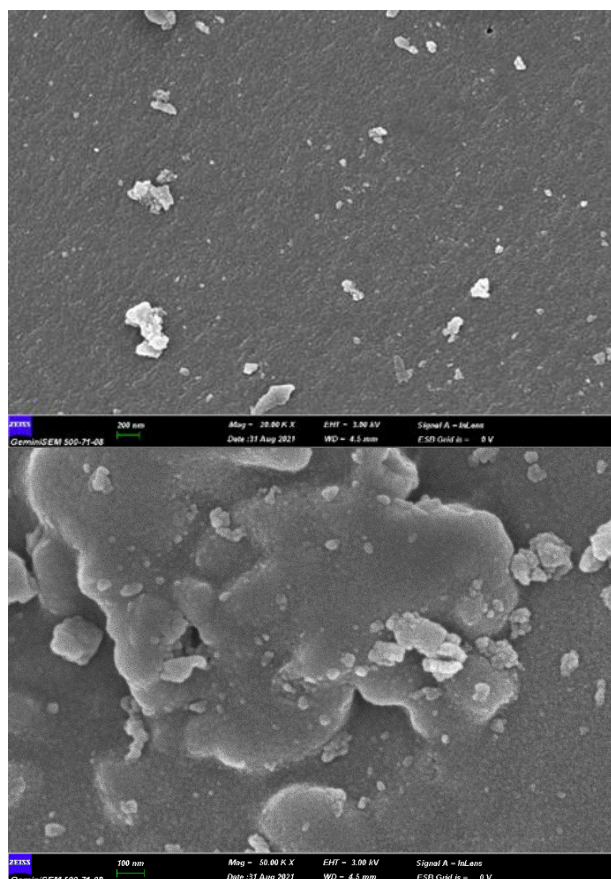
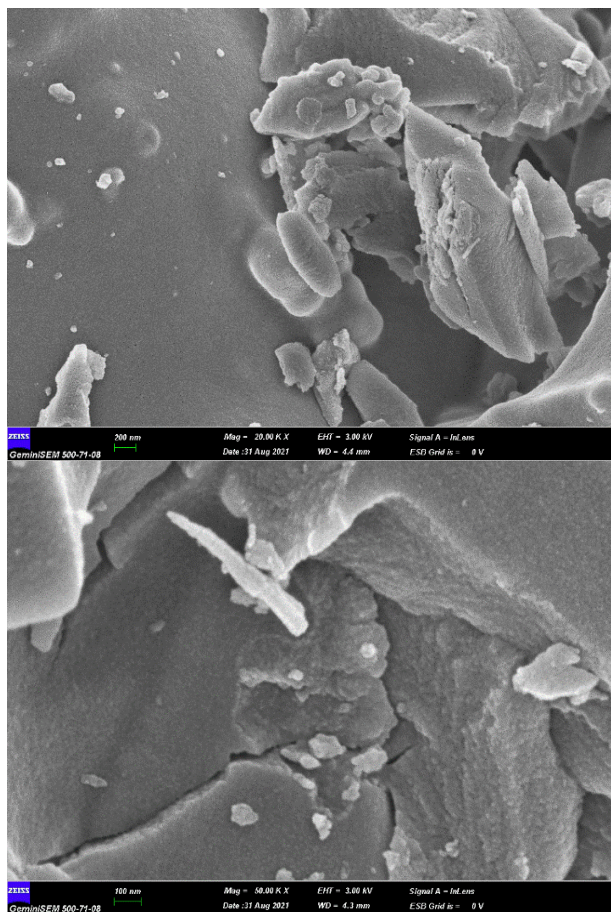


Figure 4. SEM image of mesoporous  $SiO_2$  obtained from PEG6000.

Figure 5 shows the SEM image of mesoporous SiO<sub>2</sub> prepared using PEG35000. When the images taken with 20000 and 50000 magnifications are examined, there is a homogeneous distribution. However, it is clearly seen that SiO<sub>2</sub> has a porous structure as targeted. In addition, the images demonstrate that there is no SiO<sub>2</sub> in crystalline form, instead, SiO<sub>2</sub> in amorphous structure was formed as desired. When compared with the SEM images of mesoporous SiO<sub>2</sub> prepared from PEG6000, it is understood that the materials prepared from PEG35000 are bulkier and porous.



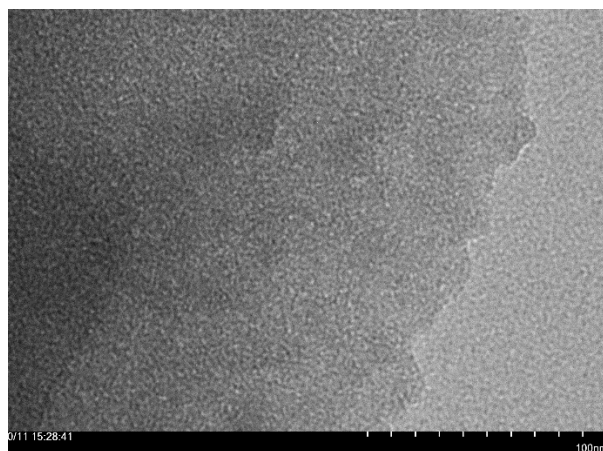
**Figure 5.** SEM image of mesoporous SiO<sub>2</sub> obtained from PEG35000.

Figure 6 displays the TEM image of mesoporous SiO<sub>2</sub> prepared from PEG6000. The image indicates that the material is porous as intended. Consistent with other analysis results, it is clear from the image that there is no crystal. This shows that the targeted amorphous porous SiO<sub>2</sub> was formed.

### 3.2. The dose-dependent cytotoxicity of mesoporous SiO<sub>2</sub> nanotube

Nano-sized silica particles are among the most commonly used and studied nanoparticles. As a kind of non-metal oxide, silica NTPs are used in many fields such as cancer therapy, enzyme

immobilization, DNA transport, and in the medical and pharmaceutical industry.<sup>21</sup>



**Figure 6.** TEM image of mesoporous SiO<sub>2</sub> obtained using PEG 6000.

Although there are so many uses of silica NTPs only a few studies exist in the literature examining their cytotoxic effects. Recently, some in vitro studies have been conducted, it has been revealed that SiO<sub>2</sub> nanoparticles have cytotoxic effects on numerous human cell types such as endothelial cell line A549 cells, EAHY96, and HaCaT keratinocytes.<sup>17,22, 23</sup> Moreover, SiO<sub>2</sub> NTPs have been found to cause proinflammatory stimulation of endothelial cells. However, an in vivo study indicated that SiO<sub>2</sub> NTPs are non-toxic and for this reason, can be used for in vivo or other biomedical applications.<sup>24</sup>

The use of MSNs has increased in recent years through their properties such as extensive pore size, high surface area, stable aqueous dispersion, good biocompatibility, and biodegradability. In this study, the efficiency of synthesized mesoporous SiO<sub>2</sub>-(PEG6000) and mesoporous SiO<sub>2</sub>-(PE35000) was investigated.

MTT assay was applied to investigate the cytotoxic effects of mesoporous SiO<sub>2</sub> NTPs. The results pointed out the cytotoxicity of SiO<sub>2</sub> NTPs on HepG2 cells increased depending on the concentration. It was also observed that both nanoparticles were not cytotoxic up to 50 µg/mL, however, they were cytotoxic after 50 µg/mL (p<0.05). It is thought that increasing intracellular SiO<sub>2</sub> concentrations are the reason why nanoparticles show toxic effects at high concentrations. Kim et al. stated that the clearance of intracellular SiO<sub>2</sub> NTPs is very fast in cancer cells. Intracellular NTPs can be reduced by NTP diffusion, cell profiling, lysosomal degradation, apoptosis, and exocytosis. Since intracellular NTPs do not reach sufficient concentrations to cause cell death, proliferation or cell death is not necessarily the main mechanism of cellular clearance of NTPs.<sup>14</sup>

Numerous studies have shown that many NTPs have potential toxicity due to their unique physical and chemical properties such as chemical purity, particle size, particle shape, zeta potential, and crystalline nature.<sup>21</sup> At the same time, many studies have indicated that the cytotoxicity of NTPs increases with concentration and time.

In this study, the amount of ROS, which is an indicator of oxidative stress, and the amount of MDA, which is a product of lipid peroxidation, were also measured. It has been shown that nanoparticles do not significantly increase MDA amounts up to concentrations of 100 µg/mL. On the other hand, it was found that the amount of ROS increased significantly even at very low NTPs concentrations. Prepared mesoporous SiO<sub>2</sub>-(PEG6000) and SiO<sub>2</sub>-(PEG35000) were applied to the HepG2 cell line at concentrations of 10, 25, 50, and 100 µg/mL. After 48

hours of incubation, ROS and MDA analyses were performed with MTT cytotoxicity test (Table 1 and Table 2). In addition, MTT, ROS and MDA results are given in Figure 7, Figure 8, and Figure 9 by comparing the results of both nanomaterials. The results of the mesoporous SiO<sub>2</sub> nanotubes in the HepG2 cell line are shown in Table 1 and Table 2. It was observed that the nanotube obtained by using PEG6000 did not show cytotoxic effect up to 25 µg/mL and did not significantly increase MDA levels even at 50 µg/mL levels. However, after 10 µg/mL concentrations, it was observed that ROS concentrations increased. It is thought that ROS increases both in response to cytotoxicity originating from the material and as a result of the defense system in the cell against a foreign substance. According to the results we obtained, it is thought that the use of nanotubes at 25-50 µg/mL concentrations is suitable for cell studies.

**Table 1.** Results from the analysis of SiO<sub>2</sub>-PEG6000 in HepG2 cell line.

	MTT (%Cell Viability)		ROS (%DCF-fluorescence, % of count)		MDA (nmol/100 mg protein)	
	Mean ± SE	p	Mean ± SE	p	Mean ± SE	p
10 µg/mL	97.15±1.14	0.928	115.25±2.93	0.341	2.94±0.43	0.996
25 µg/mL	89.51±1.50	0.073	140.75±4.66	0.001*	3.06±0.48	0.713
50 µg/mL	82.27±5.50	0.002*	226.75±7.94	0.001*	3.25±0.65	0.174
100 µg/mL	71.44±1.05	0.001*	282.50±7.85	0.001*	3.68±0.58	0.010*

\*p<0,05 is statistical significance level

**Table 2.** Results from the analysis of SiO<sub>2</sub>-PEG35000 in HepG2 cell line.

	MTT (%Cell Viability)		ROS (%DCF-fluorescence, % of count)		MDA (nmol/100 mg protein)	
	Mean ± SE	p	Mean ± SE	p	Mean ± SE	P
10 µg/mL	96.81±5.99	0.993	127.50±4.87	0.020*	3.01±0.33	0.913
25 µg/mL	87.43±2.18	0.459	165.00±5.37	0.001*	3.23±0.31	0.239
50 µg/mL	75.48±1.11	0.044*	253.75±5.56	0.001*	3.34±0.42	0.103
100 µg/mL	53.91±0.68	0.001*	311.75±8.07	0.001*	3.90±0.53	0.004*

\*p<0,05 is statistical significance level

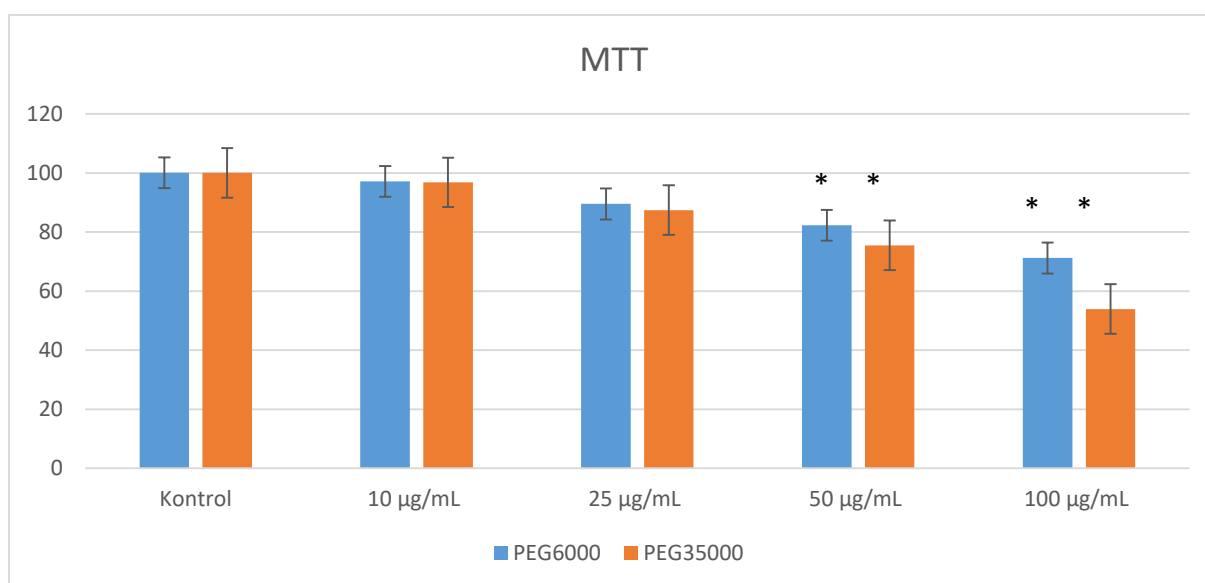


**Figure 7.** MTT results of mesoporous SiO<sub>2</sub> nanotubes.

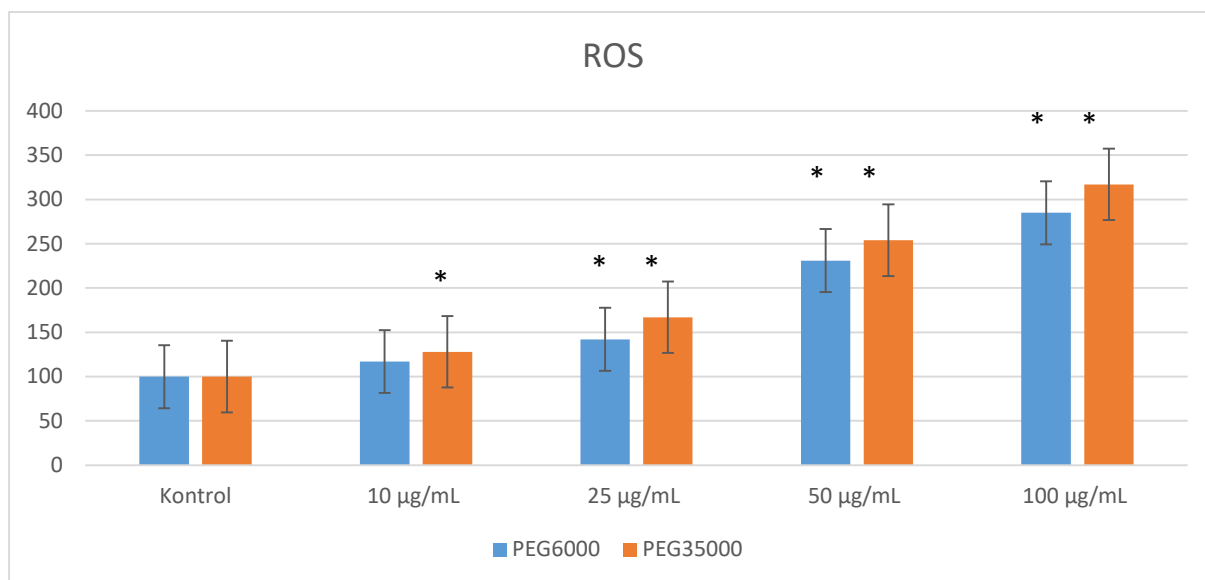


**Figure 8.** ROS results of mesoporous SiO<sub>2</sub> nanotubes

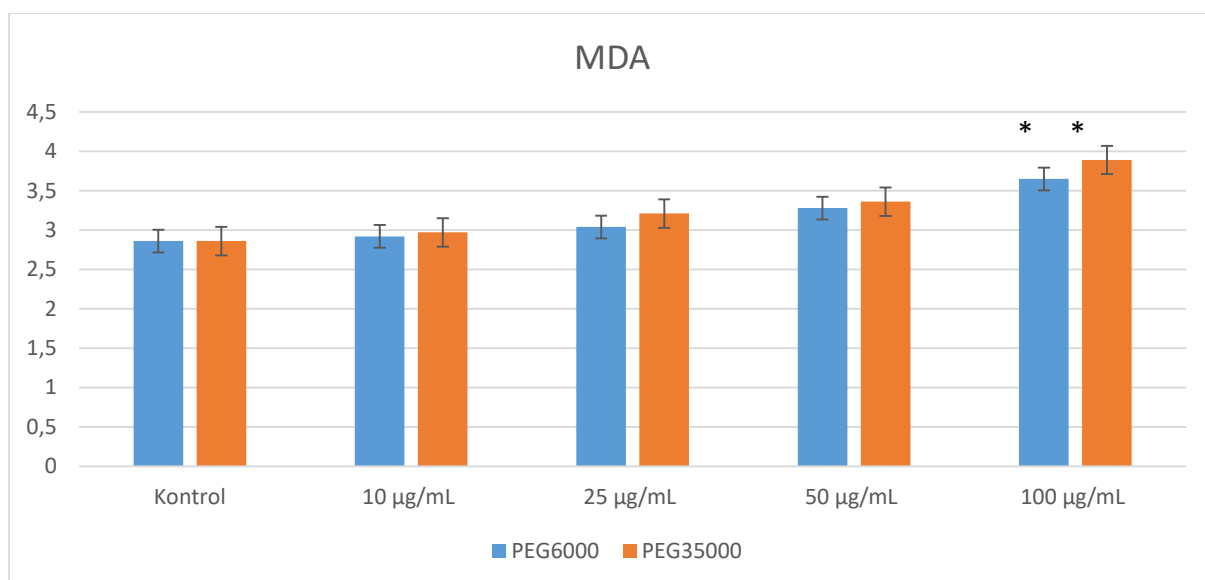


**Figure 9.** MDA results of mesoporous SiO<sub>2</sub> nanotubes.

When the results of PEG35000 were examined, it was seen that nanotubes have cytotoxic effect and significantly decrease the viability below 50 µg/mL concentrations. In addition, although it has similar effects with the PEG6000 nanotube on MDA levels, it is observed that it increases the amount of ROS statistically significantly even at a concentration of 10 µg/mL. It is seen that when both materials exceed a certain concentration, they increase lipid peroxidation in the cell walls due to their increased cytotoxic effects, thus causing an increase in MDA levels.<sup>25</sup>

When the cytotoxicity results are examined, it is seen that PEG35000 at the same concentration is more cytotoxic. This is thought to be due to the larger and

porous structure of PEG35000. When the literature is examined, there are studies showing that the cytotoxicity of nanoparticles is affected not only by concentration but also by shape and size. For example, Okla et al found that two gold nanoparticles with different sizes were not toxic at low concentrations and the nanoparticle with smaller particle size had less toxicity.<sup>26</sup> Garnez et. al. studied the cytotoxicity of two mesoporous silica nanoparticles of different sizes. In this study, they found that the larger size nanoparticle was more toxic. This increased cytotoxicity is thought to be due to increased shell size, compaction/lack of voids, or large shape that can damage cell membranes and affect both cellular uptake and viability.<sup>27</sup>

Gupta et al. emphasized that the ideal size of nanoparticles to be used in drug delivery studies should be between 10-100 nm. In this way, the drug will be able to enter the cell and, due to its size, the drug will not be expelled by the resistance pumps.<sup>28</sup> As a matter of fact, in our study, both nanotubes were in this range. In this way, our nanomaterials will be able to enter the cell with the drug and show their effect by controlled drug release, thus making them a good candidate for drug transport studies. In a study conducted with Fe<sub>3</sub>O<sub>4</sub> magnetic nanoparticles, it was shown that nanomaterials synthesized between 20-50 nm provide serious advantages on cancerous cells and kill cancerous cells even at lower concentrations by providing significant reductions in drug resistance gene expressions.<sup>29</sup>

Oxidative stress caused by nanomaterials has been shown in many studies.<sup>21</sup> ROS production followed by oxidative stress generation is the predominant mechanism leading to nanotoxicity, including carcinogenesis, apoptosis, genotoxicity and DNA damage. In addition, the main site of cellular ROS production is the mitochondria. Any functional and structural defect can result in mitochondrial ROS accumulation, which is the essential inducer of apoptosis.<sup>30</sup> Similar to these results, Liang et al. showed that ROS and oxidative stress-related mediators increased with increasing SiO<sub>2</sub> nanoparticle concentrations.<sup>21</sup> It is thought to cause cytotoxicity by intracellular accumulation of SiO<sub>2</sub>. The fact that NTPs using PEG35000 cause ROS production at lower concentrations shows that particle size affects ROS. Increased particle sizes are more difficult to get out of the cell, causing SiO<sub>2</sub> NTPs to accumulate faster inside the cell.

This study shows the first report on synthesis of these molecules. Therefore, the full elucidation of the cytotoxic effects of these molecules and their effects on the oxidative stress mechanism will shed light on drug studies based on these molecules.

#### 4. CONCLUSION

In this study, mesoporous SiO<sub>2</sub> nanoparticles were synthesized by a method that has not been used before. The cytotoxic effects of these synthesized materials in drug transport studies, where they are frequently used, were examined in the HEPG2 cell line. It was found that both nanomaterials were not cytotoxic at 25 µg/mL concentrations and started to show toxic effects after 50 µg/mL. This study shows that the toxic effects of mesoporous increased depending on the concentration. The results show that these mesoporous nanomaterials can be used as a good drug carrier at certain concentrations because they are inexpensive, safe, and easy to synthesize.

#### ACKNOWLEDGEMENTS

I would like to thank Prof Dr Sevim KÖSE from Karadeniz Technical University for the editing and comments in my article.

#### Ethics Statements

There is no problem in terms of research and publication ethics.

#### Conflict of interests

I declares that there is no a conflict of interest with any person, institute, company, etc.

#### REFERENCES

1. IARC Working Group. Silica Dust, Crystalline, in The Form Of Quartz Or Cristobalite. <https://www.ncbi.nlm.nih.gov/books/NBK304370/> (accessed 10.08.2024).
2. Güler, E.; Uğur, G.; Uğur, Ş.; Güler, M. *Chin. J. Phys.* **2020**, *65*, 472-480.
3. Zhang, F.-F.; Wan, Q.; Li, C.-X.; Wang, X.-L.; Zhu, Z.-Q.; Xian, Y.-Z.; Jin, L.-T.; Yamamoto, K. *Anal Bioanal Chem Res* **2004**, *380* (4), 637-642.
4. Lin, W.; Huang, Y.-w.; Zhou, X.-D.; Ma, Y. *Toxicol Appl Pharmacol* **2006**, *217* (3), 252-259.
5. Cicha, I.; Priefer, R.; Severino, P.; Souto, E. B.; Jain, S. *Biomolecules* **2022**, *12* (9), 1198-1198.
6. Pollard, K. M. *Front. Immunol.* **2016**, *7*.
7. Mossman, B. T.; Glenn, R. E. *Crit. Rev. Toxicol.* **2013**, *43* (8), 632-660.
8. Leung, C. C.; Yu, I. T. S.; Chen, W. *Lancet* **2012**, *379* (9830), 2008-2018.
9. Peters, K.; Unger, R. E.; Kirkpatrick, C. J.; Gatti, A. M.; Monari, E. *J. Mater. Sci.: Mater. Med.* **2004**, *15* (4), 321-325.
10. Chen, Y.; Chen, J.; Dong, J.; Jin, Y. *Toxicol. Ind. Health.* **2004**, *20* (1-5), 21-27.
11. Chen, M.; Vonmikecz, A. *Exp. Cell Res.* **2005**, *305* (1), 51-62.
12. Xie, G.; Sun, J.; Zhong, G.; Shi, L.; Zhang, D. *Arch Toxicol* **2010**, *84* (3), 183-190.
13. Chauhan, S.; Manivasagam, G.; Kumar, P.; Ambasta, R. K. *Pharm. Nanotechnol.* **2019**, *6* (4), 245-252.



14. Kim, I. Y.; Kwak, M.; Kim, J.; Lee, T. G.; Heo, M. B. *Nanomaterials (Basel)* **2022**, *12* (6).
15. Valic, M. S.; Zheng, G. *Theranostics* **2019**, *9* (11), 3365-3387.
16. Wang, J.; Shen, Y.; Bai, L.; Lv, D.; Zhang, A.; Miao, F.; Tang, M.; Zhang, J. *Colloids Surf B Biointerfaces* **2014**, *116*, 334-42.
17. Yang, X.; Liu, J.; He, H.; Zhou, L.; Gong, C.; Wang, X.; Yang, L.; Yuan, J.; Huang, H.; He, L.; Zhang, B.; Zhuang, Z. *Part Fibre Toxicol* **2010**, *7*, 1.
18. Wang, H.; Joseph, J. A. *Free Radic Biol Med* **1999**, *27* (5-6), 612-6.
19. Jain, S. K.; McVie, R.; Duett, J.; Herbst, J. J. *Diabetes* **1989**, *38* (12), 1539-43.
20. Dubey, R. S.; Rajesh, Y. B. R. D.; More, M. A. *Mater. Today* **2015**, *2* (4-5), 3575-3579.
21. Liang, H.; Jin, C.; Tang, Y.; Wang, F.; Ma, C.; Yang, Y. *J Appl Toxicol* **2014**, *34* (4), 367-72.
22. Lison, D.; Thomassen, L. C.; Rabolli, V.; Gonzalez, L.; Napierska, D.; Seo, J. W.; Kirsch-Volders, M.; Hoet, P.; Kirschhock, C. E.; Martens, J. A. *Toxicol Sci* **2008**, *104* (1), 155-62.
23. Napierska, D.; Thomassen, L. C.; Rabolli, V.; Lison, D.; Gonzalez, L.; Kirsch-Volders, M.; Martens, J. A.; Hoet, P. H. *Small* **2009**, *5* (7), 846-53.
24. Jin, Y.; Kannan, S.; Wu, M.; Zhao, J. X. *Chem Res Toxicol* **2007**, *20* (8), 1126-33.
25. Lin, W.; Huang, Y. W.; Zhou, X. D.; Ma, Y. *Toxicol Appl Pharmacol* **2006**, *217* (3), 252-9.
26. Okła, E.; Białocki, P.; Kędzierska, M.; Pędziwiatr-Werbicka, E.; Miłowska, K.; Takvor, S.; Gómez, R.; de la Mata, F. J.; Bryszewska, M.; Ionov, M. *Int J Mol Sci* **2023**, *24* (7).
27. Pérez-Garnes, M.; Gutiérrez-Salmerón, M.; Morales, V.; Chocarro-Calvo, A.; Sanz, R.; García-Jiménez, C.; García-Muñoz, R. A. *Mater Sci Eng C Mater Biol Appl* **2020**, *112*, 110935.
28. Gupta, A. K.; Gupta, M. *Biomaterials* **2005**, *26* (18), 3995-4021.
29. Ulusal, H.; Ulusal, F.; Bozdayi, M. A.; Guzel, B.; Taysi, S.; Tarakcioglu, M. *Int. J. Chem. Technol* **2022**.
30. Li, X.; Kang, B.; Eom, Y.; Zhong, J.; Lee, H. K.; Kim, H. M.; Song, J. S. *Sci Rep* **2022**, *12* (1), 155.